

Human Fingernail Segmentation

¹Kumuda N S, ^{1,1}Dinesh M S

University of Mysore
 PET Research Center, PES College of Engineering
 Mandya, Karnataka, India
¹kumuda_roy@yahoo.co.in

Abstract — In this paper we present a method for segmentation of fingernail patterns and differentiate them as distinct nail parts; fingernail plate with lunula and distal free edge of nail plate. In the research work, focus is on fixed area of the fingernail plate plus lunula, as it remains unchanged in structure, where as the distal nail edge extends and changes in structure over a period of time. In order to segment fingernail parts, we have devised an algorithm that automatically separates unchanging region of fingernail plate from free distal edge of nail structure. The fingernail plate that includes lunula within (may or may not be prominently present in fingernails), is used as biometric in our advance study. Theory suggests, every fingernail within finger formation comprises of the brightest regions amongst the captured finger data set (in our system). Proposed method is of two stages. In first stage, color image is converted to gray scale and contrast enhancement is applied using adaptive histogram equalization. In second stage, we perform segmentation using watershed method that exercises maxima and minima properties of marker controlled watershed principles. In order to verify the results of the algorithm, we have constructed a confusion matrix where evaluation has been done with ground truth. Additionally, the segmented object's from both the methods is considered for quality metrics assessment. Similarity accuracy between the ground truth and watershed result is 84.0% correctness for fingernail plate. Initial fingernail segmentation results are promising, supporting its use for biometric application.

Keywords— *Fingernail plate, dista free edge, lunulae, contrast-limited adaptive histogram equalization, marker controlled watershed segmentation, ground truth, region properties, confusion matrix, jaccard meric.*

I. INTRODUCTION

Human hands and fingers are considered as one of the primary tools for interacting with every physical object the individual wishes to. One of the current applications of fingernail is to use display screens to enhance interactions with touch screen sensors. Although there are other advantages of it in biometric recognition, we have very few fingernail based real world applications addressing the problems. In the recent past, interestingly, it has also been a topic of discussion both in theory and survey intended for computer vision, robotics and implementations in Artificial Intelligence (AI) resembling pattern recognition, digital image processing and so on.

It is also evident from literature that not many uses of fingernails features have been explored. Its applications are not made use of and their advantages are not yet focused. However, gradually, the fingernails recognition as a biometric is gaining support and acceptance in significant circumstances that support segmentation for classification or identification in digital system [8, 13]. Hence, we believe to have a scope for our research method in this attempt.

In this paper, we introduce biometric fingernails images as new patterns and define segmentation method in recognition technology [2]. The method depends on structural characteristics of objects that may change over time or need not. Since the fingernails grow, the nail plate region automatically retains its basic structure for itself over a period of time, unless accidentally damaged. Hence, in contrast to growing distal free nails, it is the actual nail plate textures that are naturally present without change in shape probably with minor variations in outline. As a result, it is presumed to be helpful in the construction of more acceptable attributes for recognition systems. We propose to illustrate to locate the following regions of fingernail features (major); distal free edge, nail plate and lunula (smaller sub-objects) at the bottom of the nail may appear or may not at random in different fingers of an individual as shown in Fig. 2.

Digital image quality and clarity exhibit different character dependability amongst various image processing operations. Accordingly, the clarity of images play extremely important responsibility. Separating free nail growth region and nail bed of the finger structure is a fairly difficult task, as the structural arrangement and sizes can vary from person to person. The color combination exhibits drastic variance with changeable skin complexion over the range of population across. Which means to say that the problem at one hand is different physical combination of fingernail structures while on the other it is image variation during biometric acquisition. Various finger objects possess free nail edges which have bright pixels with brittle structure that is clearly differentiable, while several cases that are moderately differentiable have less contrast and in other cases there is slight difference present between finger skin and fingernail structure at lateral edges of fingernail folds with soft, thin nail formation [1, 17]. The differences in bright, more bright, just bright has to be considered though very difficult and paid more attention while identifying the finger

nail structure into its sub parts. As a result, this affects the system evaluation of fingernail parts recognition.

The general idea of quality measure of segmented results is basically to help in constructing and understanding of the overall performance of the procedure followed by its outcome. This is to arrive at good segmentation results with careful region approximation of complete fingernail pattern detection [12]. The process marginally relate to identified, manipulated and improved objects by repetition of the module when required. This shows up in the segmentation process (stages of marker controlled region selection). The excess resources beyond our level of knowledge (i.e., Images inclined in 3rd dimension) for assessment is not very helpful. Throughout the development of this method, several approaches were attempted, with varying degrees of success for retrieving all regions separately including the background. Thus, the algorithm characterizes the robustness by justifying the marker based scale-space regions [6, 7].

The remaining part of the paper is organized as follows: Section II - briefly presents the biometric data collection and feasibility study of its patterns, which comprise of objectives for finger nail structure. Section III - contains all points of watershed approach for segmentation including algorithm and feature extraction. Section IV - shows experimental results for evaluation. Finally, Section V - concludes with its results for an outcome in the future (perspectives).

II. FINGERNAIL DATA

A. Human Fingernails

It is known that fingernails are made of tough protein called keratin that appears very light in color (range of pink shades) in all most all humans. The supportive bone structure, in half-moon shape is referred to as Lunula is seen at the bottom of the nail (appears randomly in different fingers). It is this group of cells that produce keratin and other living cells. The living cells as they die are then pushed forward by newer cells to merge with the keratin and become flat, stiff part of nail plate. It is the largest part of the nail and is made up of dead cells till the free edge of fingernails; as labeled in Fig. 1. (a, b). Manual approaches to fingernail selection and its sub parts as smaller objects are affected structurally. This is due to human selection and opinions, most of the time fallow psychological dependence rather than physical measure. Hence computer assisted process (digital) for fingernail extraction through biometric analysis is suggested.

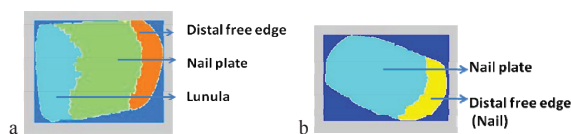


Fig. 1. Fingernail structure; (a) with lunula, (b) without lunula.

B. Data Collection

In our research work we focus approximately on a small set of 200 images from different fingers for preliminary experimentation of fingernail part segmentation. Among

variety of fingernail images collected with the help of in-house setup, overall 200 images appeared with completely grown distal nail edges. These fingernail images were considered relevant for pattern segmentation as per the planned method. Image in Fig. 2(e) has fingernail plate with lunula pattern which is prominently visible. While Fig. 2 (a, b) images do not have the lunula as intrinsic part of fingernail plate. Where as in Fig. 2(c, d) lunula is faintly present as part of fingernail plate region (not able to distinguish).

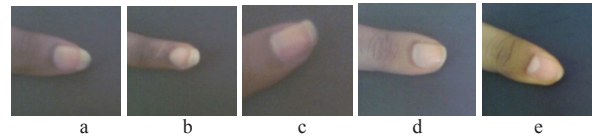


Fig. 2. Data collection shows variations in fingernail structure and distal free edges (in available data set) ; (a)-(e) are few image examples.

C. Objective

The purpose of the proposed approach is to identify fingernail parts as correctly as possible from digitally acquired finger images, with many inherent errors exhibiting variations in image patterns [1]. We also demonstrate that these images of the finger nails constitute various pattern attributes for a recognition system and is as shown in Fig. 3 (expected fingernail features as sub-regions).



Fig. 3. (a) Fingernail plate with distal free edge, (b) complete fingernail, (c) fingernail plate separated from distal free edge.

III. PROPOSED METHOD

We, in this paper suggest a modern and robust process that has helped in subjective image enhancement feature detection. Besides, automatic and relaxed fingernail object recognition for fingernail parts selection. The novel method combines; (i) Contrast-limited Adaptive Histogram Equalization followed by global thresholding. (ii) Morphological operations for noise corrections [9]. (iii) lastly multi-step marker controlled watershed transformation for fingernail pattern segmentation.

A. Preprocessing

In this step, each of the finger images is cropped to 600 x 600 pixels in size before testing. The colour finger images are read one by one to convert to gray scale before enhancing its contrast level. Pre-processing of the “desired” regions depends on the objects of interest. Fingernails in Fig. 1, clearly illustrates the need to having a global parameter to recognize image objects in our implementation. Even if there is a reason to decide on a single global parameter for every image, it exists for background thresholding with foreground as different unit (finger parts as objects of importance). But in the present case, with “desired” recognition system of the fingernail image parts, it needs enhancement of every area

iteratively. For this reason, we apply Contrast-Limited Adaptive Histogram Equalization (CLAHE).

B. Segmentation

The above preprocessing step supports the use watershed approach. Marker controlled watershed clearly separates homogeneous gray-tones of finger images considering its textures as topographic surface (markers). The transformation is often applied to these kinds of problems [11, 15]. The method finds “catchment basins” and “watershed ridge lines” in an image by treating it as a surface where light pixels are high and dark pixels are low areas. Segmentation process is as follows:

- The contrast of images is enhanced to avoid noise amplification in the intensity adjusted images [5]. At any instant, it is essential to deal with inherent, non uniform lighting effects as much clearly as possible to obtain the said features. Determining the real clip limit from the normalized value is a necessity (gray image).
- The enhanced image is thresholded using Otsu's method which involves iterating through all the possible threshold values, calculating spread measure in an optimal manner. In the binary image, however, there is a possibility of gradients by small intensity variations mainly due to random *noise* (bright pixel regions identified in neighbourhood) [12]. These unexpected random blob areas are required to be avoided as it leads to over segmentation by the presence of many local minima. To decrease this effect of severe over segmentation of watershed transformations [11], the morphological operations is applied for regions filling of small holes in regions connecting boundary pixels. The calculations of areas and boundaries for best results are obtained by marking the patterns before segmentation and watershed transformation (mask image).
- Marker transformation of the gradient image is set of pixel points as represented in the function f . It is viewed as topographic surface S , having the highest Gradient Magnitude Intensity (GMI) pixel like watershed lines as region boundaries. Pixels with Local Intensity Minimum (LIM) are the common watershed lines. Pixels with a common minimum appear like segment sink as basins represented by Eq. 1. The lighter gray values in the function at point x , represents the higher altitude of the corresponding point on the surface. M is a minima of f and is made of all possible connected components of regions M_i in f . An imposed minima where the blobs are detected by the watershed transform [4, 10] (marker image).

$$\forall s_i(x_i, f(x_i)), s_j(x_j, f(x_j)) \quad i \geq j \Leftrightarrow f(x_i) \geq f(x_j) \quad (1)$$

- The image *intensity minima transform* identifies valleys deeper than a particular threshold to change a

valley's pixel to contain only zeros (deepest possible valley for uint8 images). The location of the regions is important rather than the size of region in the image. All regions containing an imposed minima are detected by the watershed's transform.

- To sum up the steps of watershed algorithm adopted; objects of interest are identification with pixel correlation, boundary edge detection through intensity difference, morphological clearing of randomly spread noise, pulling out similar pattern patches [9, 14] as regions segmented. Its connected values are conveniently labeled to further break them into smaller sub-regions. Binary areas are extracted to measure shape and region properties (resultant segmented objects).

In Fig. 4, the flow diagram of the proposed algorithm, output results at every stage is as follows.

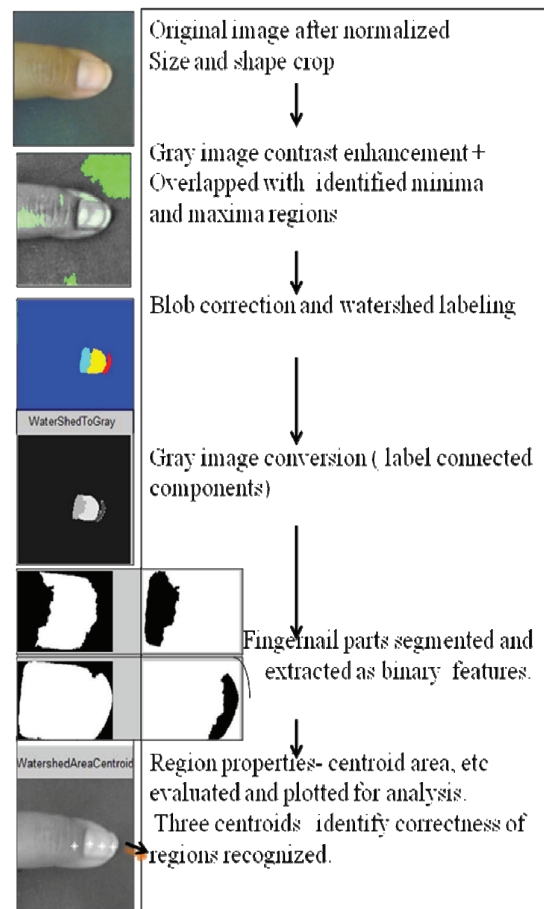


Fig. 4. Four areas and centroid plot of proposed method; fingernail plate, distal free edge, lunula and image back ground.

Because of the variation in contrast of image objects (within the data set), both nail plate and distal free edge area are recognized as one object. To overcome this problem, watershed segmentation procedure is carried out again to obtain distal free edge area separately. During algorithm












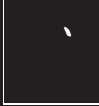




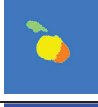























execution, a maximum of 2-iterations are considered. In the first iteration, 0.44% images and in the second iteration, 51% images were correctly segmented all parts of fingernail plate (removing distal free nail). The remaining 0.05% fingernail images regions were not correctly identified.

C. Ground Truth

Manual region segmentation for all 200 finger images was carried out for complete fingernail plate and distal (free) nail edge separately. Some of the examples are given within column 4-5 in Table I, as an outcome of the method [3, 7].

D. Feature Extraction

TABLE I. SAMPLE FEATURES OF FEW DATA IMGES FOR MARKER WATERSHED SEGMENTATION AND GROUND TRUTH METHODS

Sr No	Watershed Fingernail	Watershed Distal Nail	Ground Truth Fingernail	Ground Truth Distal Nail	Match % Range
1					91-100
2					91-100
3					61-70
4					71-80
5					91-90
6					71-80
7					71-80
8					81-90
9					71-80
10					91-100

The data set showed that, only 10 people had their distal nail edges grown in 'n' different fingers. Therefore from the related finger image data set, 50% of images were selected for training and 50% of images for testing. With 5 samples supporting the data set for every finger of every person, the watershed segmentation method is implemented [7]. Fingernail plate results of ground truth in comparison to watershed segmentation is shown in Table I.

IV. SUPERVISED EVALUATION

In this step we present experimental results of our algorithm, including comparison of the segmentation results obtained with two alternative segmentations; Ground truth [19, 20], and marker controlled watershed [10, 15]. They are chosen because they represent absolute and ground truth methods in image segmentation. The implementation of the algorithm is in comparison to quantitative study of quality segmentation. Purpose of accuracy measure is to define as to how well the automated segmentation output agrees with human segmentation perception.

A. Segmented Regions Assessment

1) *Confusion matrix*: is tabulated in Table II which shows segmented region analysis of both the algorithm results. The ground truth results is *composed* of only three (*n*) segments. While automatically segmented output images are *expected* to contain three (*m*) segments if correctly identified [19]. The confusion matrix shows common image regions between resultant pair of segmented images of both the methods applied (in terms of number of pixels). M_{ij} represents the common number of pixels that belongs to the segment *i* of the watershed object W_i and segment *j* refers to ground truth object GT_j with agreeing matrix dimensions.

TABLE II. CONFUSION MATRIX

i/j	Confusion matrix tabulated for 5th row segmented data regions (images) as shown in TABLE I.		
	GT_1	GT_2	GT_3
W_1	$M_{11}=18200$	$M_{12}=1799$	$M_{13}=0$
W_2	$M_{21}=330$	$M_{22}=5338$	$M_{23}=0$
W_3	$M_{31}=9$	$M_{32}=0$	$M_{33}=336462$

In Table II: M_{11} represents common area pixel count of two fingernail plate region areas. M_{22} is the common area pixel count for distal free edges. And M_{33} is the common area pixel count for background region from both ground truth and watershed segmented methods [17]. Some more segmented output image results showing comparison of both the methods are included in Table I.

2) *Similarity measure*: In order to determine similarity measure, the following numbers are computed:

a) p_{11} : number of pixels that belongs to same segment in watershed segmented image and the ground truth.

b) p_{10} : number of pixels that belongs to same segment in watershed segmented image but not in ground truth.

c) $p01$: number of pixels that belongs to same segment in ground truth but not in watershed segmented image.

d) $p00$: number of pixels which are in different region both in ground truth and watershed segmented image.

The following Eq. 2-5 compute, $p11$, $p10$, $p01$, $p00$ information respectively:

$$p_{11} = \frac{1}{2} \left[\sum_{i=1}^k \sum_{j=i}^l M_{ij}^2 - p \right] \quad (2)$$

$$p_{10} = \frac{1}{2} \left[\sum_{i=1}^k |GT_i|^2 - \sum_{i=1}^k \sum_{j=i}^l M_{ij}^2 \right] \quad (3)$$

$$p_{01} = \frac{1}{2} \left[\sum_{j=1}^l |W_j|^2 - \sum_{i=1}^k \sum_{j=i}^l M_{ij}^2 \right] \quad (4)$$

$$p_{00} = \frac{n(n-1)}{2} - p_{11} - p_{10} - p_{01} \quad (5)$$

The segmented image quality metrics are related to the difference between two images; the original object (ground truth segmentation) and automatically detected object (watershed segmentation). The column's measures gives us the total number of correctly matched, incorrectly matched, partially matched or mismatched results for the corresponding data items between the two feature sets [18].

B. Jaccard Distance Measure

The Jaccard similarity coefficient measure is used for statistical comparison to combine dissimilarity and similarity overlap of two relevant object sets (objects of ground truth and watershed method). The Jaccard coefficient measures the similarity of overlap between finite samples (x , y) and is defined as the area size of the intersection (common area identified) divided by the area size of the union (over all area identified) of the two corresponding object data sets.

Jaccard distance (index) for set of resulting binary data is used to judge the outcome of fingernail parts segmentation. There is a possibility of implementation which can work on non-binary data as long as the information matches are exact in units and/or in measures [19].

$$jac(x, y) = \frac{|x \cap y|}{|x| + |y| - |x \cap y|} \quad (6)$$

Jaccard similarity by Eq. 6 and dissimilarity measure by Eq. 7 is calculated between every sample data set. Jaccard index which is complementary to the Jaccard similarity coefficient, is also obtained by subtracting the Jaccard coefficient from 1 as the range lies between 0-1. Object images of ground truth and watershed method should be

numerical; ideally integer with foreground regions having values of 1, 2, 3, ... N etc. So that we create binary images out of this to evaluate each foreground area separately. Later similarity of asymmetric binary attributes of object structures is more easily measured by doing $1 - \text{the Jaccard distance}$. We get to the Jaccard index as follows:

$$J_g(x, y) = 1 - jac(x, y) = 1 - |x \cap y| / |x \cup y| \quad (7)$$

C. Region Based Measures

The parameters like area, centroid of that area are calculated to check for overlapping regions of ground truth nail plate to marker watershed segmented area in colors in Fig 5(b). The major axis and minor axis are evaluated for shape comparison of the two segmented areas [16]. Bounding box gives filled area measure as a cross validation that is added measure for the nail plate region and free nail edge feature recognized both in terms of area limit specification and shape which is represented in blue and yellow colors in Fig. 5(b).

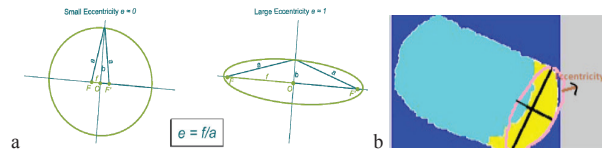


Fig. 5, Parameter evaluation w. r. t., minor axis, major axis; (a) measure f eccentricity of area shape, (b) bounding box area limits.

The estimate $e = f / b$ as explained in Fig. 5(a), measures eccentricity from roundness, to determine elongated shape attribute. This proves distal free nails are longer in shape and fingernail plates are not so stretched out in shapes.

D. Result Analysis

The statistical accuracy evaluation for area and eccentricity of fingernail plates ranges between 75-95%. Area measure comparison is carried out for results of both the methods and is as shown in Fig. 6, (with green curve-ground truth, yellow curve-watershed segmentation representation):

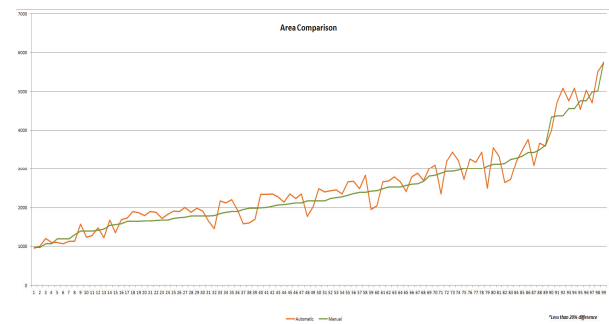


Fig. 6, Comparative graph analysis for test data set (results of both ground truth and watershed method); area measure.

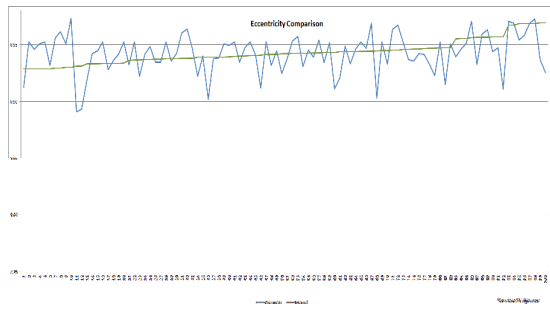


Fig. 7. Comparative graph analysis for test data set (results of both ground truth and watershed method); eccentricity measure.

Eccentricity comparison measures is as in Fig. 7, (green curve-ground truth, blue curve-watershed segmentation). At the same time eccentricity similarity for distal free edge was calculated. Result shows above 92-97% match. Eccentricity measure also suggests that distal free edge is mostly oval in structure different from fingernail plate which can be either elliptical or rectangular.

The result of comparison between ground truth and watershed segmentation for all the 200 data points (50% training and 50% test) are tabulated in Table III. Following 61-80, 81-100 range considered; 1) the evaluation results are correctly recognizing around 160 (84%) images above 80% accuracy for fingernail plate area. 2) And for distal free edge it is 149 (78.4%) images above 80% accuracy. Lastly, 5.7% fingernail plate and 4.7% outlier images were treated.

TABLE III. FINGERNAIL PLATE SEGMENTATION ACCURACY COMPUTED IN DIFFERENT RANGES

Percentage Conformity		
Accuracy Range (%)	Distal Nail Edge	Nail Plate
100-80	149	160
80-60	41	30
Total Images	190	190

CONCLUSION

In, this paper, the marker controlled watershed method is employed for segmentation of interested fingernail objects. Segmentation process shows encouraging results with more than 80% good region of interest extraction and helps measure its features. Consequently, the result estimation shows consistency in quality of nail plate region segmented from all images with difference in object orientations. However the process of separating fingernail parts has helped us to do away with the distal free edge and consider only the fixed nail plate region. And we plan to extend the segmentation methodology for nail biometric identification. We have also programmed to increase the fingernail images in the dataset for our future experimentation techniques. The proposed algorithm is considered robust as the results are invariant to orientation, scaling and translation.

REFERENCES

- [1] P. Baden, "The physical properties of nail," *Journal of investigative dermatology*, vol. 55, no. 2, pp. 115-122, 1970.
- [2] Asano, T. and Yokoya, N., "Image segmentation scheme for low level computer vision," *Pattern Recognition*, 14, 267-273, 1981.
- [3] Diggle, P.J., *Statistical Analysis of Spatial Point Patterns*. Academic Press, London, 1983.
- [4] Borgfors G., "Distance transformations in digital images", *Computer Vision, Graphics Image Processing*, 34, 344-371, 1986.
- [5] Glasbey, C.A. "An analysis of histogram-based thresholding algorithms," *CVGIP: Graphical Models and Image Processing*, 55, 532-537, 1993.
- [6] Lindeberg, Tony, *Scale-Space Theory in Computer Vision*, Kluwer Academic Publishers, ISBN 0-7923-9418-6, 1994.
- [7] Tony Lindeberg, "Feature detection with automatic scale selection," *International Journal of Computer Vision*, vol. 30, Issue 2, pp.77-116, 1998.
- [8] A. A. Green, M. Berman, P. Switzer, M. D. Craig, "A transformation for ordering multispectral data in terms of image quality with implications for noise removal," *IEEE Transactions on Geo-science and Remote Sensing*. vol. 26, pp. 65-74, 1998.
- [9] Y. Zhu, T. Tan, and Y. Wang, "Biometric personal identification system based on iris pattern," *Chinese Patent Application*, No. 9911025.6, 1999.
- [10] Pierre Soille, "Morphological image analysis: principles and applications," Springer-Verlag, pp. 170-171, 1999.
- [11] George J. Grevera, "Distance transform algorithms and their implementation and evaluation," *Saint Joseph's University Philadelphia, Pennsylvania, USA*, pp 33-60, 2007.
- [12] Rafel C Gonzalez and Richard E Woods, *Digital Image Processing*, Pearson Education India, 2009.
- [13] Diogo Kuiaski, Hugo Vieira Neto, Gustavo Borba, Humberto Gamba, "A study of the effect of illumination conditions and color spaces on skin segmentation," *Computer Graphics and Image Processing (SIBGRAPI)*, IEEE CS, pp. 245-252, 2009.
- [14] D. Chai, A. Bouzerdoum, "A Bayesian approach to skin color classification in YCbCr color space," *IEEE TENCON00*, vol. 2 pp. 421-424, 2000.
- [15] S. T. Acton, D. P. Mukherjee. "Scale space classification using area morphology", *Image Processing*, IEEE Transactions, pp. 623-635, vol.9, Issue 4, 2000.
- [16] Jain, A.K., Duin, P.W., "Pattern analysis and machine intelligence," In: *IEEE Transactions on* vol. 22(1), pp.4-37, 2000.
- [17] H.G. Lewis, and M. Brown, "A generalized confusion matrix for assessing area estimates from remotely sensed data," *International Journal of Remote Sensing*, vol. 22, Issue 16, pp 3223-3235, Nov. 2010.
- [18] S. L. Phung, A. Bouzerdoum, and D. Chai, "Skin segmentation using color pixel classification: analysis and comparison," *IEEE Trans. Pattern Anal. Mach. Intell.*, vol. 27, no. 1, pp. 148-154, Jan. 2005.
- [19] Christopher, M. Bishop, *Pattern Recognition and Machine Learning*, 2007.
- [20] D. Ramanan, "Using segmentation to verify object hypotheses," In *CVPR*, pages 1-8, 2007.